Absorption Measurements of the Principle Series Lines of Cs Broadened by Xe

J. Lorenzen and K. Niemax

Institut für Experimentalphysik der Universität Kiel

(Z. Naturforsch. **32 a**, 853–862 [1977]; received May 16, 1977)

The absorption coefficients of the statistical wings of the Cs principal series lines $6\,^2S_{1/2}-n\,^2P_{3/2}$ ($6 \leqq n \leqq 10$) and $6\,^2S_{1/2}-n\,^2P_{1/2}$ ($6 \leqq n \leqq 9$) perturbed by Xe have been measured quantitatively The results are compared with quasistatic line wings calculated from the interatomic Cs–Xe potentials of Baylis [1] and Pascale and Vandeplanque [2]. In the far wings of the higher lines of the series indications of many-body interaction were found. Furthermore the behaviour of the shift of all principal series lines up to the 23rd member was investigated in the density region between 1.63×10^{18} and 1.9×10^{19} Xe atoms per cm^{-3}.

1. Introduction

Line broadening is a very useful tool for obtaining information about the interaction of colliding atoms. Especially the far and the very far line wings are closely related to the interaction potentials through the quasistatic theory [3]. For alkali-noble gas systems it was shown first [4] that the potentials can be determined from a line broadening experiment if the difference potential (difference of excited and ground state potential) is a monotonic function of the interatomic distance. If this condition is not fulfilled, an assumption of the potential forms, for example a Lennard-Jones form (C_6, C_{12}), has to be made [5]. Fitting the Lennard-Jones potentials of the ground and excited states to the conditions of experimental line wings, the intercompared with quasistatic wings calculated from adiabatic potentials by Baylis [1].

On the other hand a quantitative measurement of the statistical wings is very useful for checking realistic theoretical potentials. This was first done by Chen and Phelps [6]. In their paper the measured wings of Cs resonance lines broadened by Ar were compared with quasistatic wings which were calculated with the help of the adiabatic potentials of Baylis [1].

It is less favourable to get information about the interatomic interaction from the impact broadened line centre. A direct determination as in the case of the statistical wings is not possible. Instead the measurement of the broadening and the shift of the lines which, are related primarily to the long-range interaction region, can be used to check available theoretical adiabatic potentials [7] or to determine interaction constants for assumed model potentials, for example for Lennard-Jones potentials [8, 9].

This paper reports on quantitative measurements of the statistical wings of Cs principal series lines broadened by Xe. In order to check the quality of the theoretical adiabatic potentials of the Cs-Xe system calculated by Baylis [1] and Pascale and Vandeplanque [2] a comparison between the measured statistical and the theoretical quasistatic line wings is given.

In the second part of this work we report on the behaviour of the shift of the Cs principal series lines caused by Xe. In addition to the different shift of the lower members of the series (well described by the impact theory) and the nearly uniform shift of the higher members (Fermi theory [10]) the transition region between both theories was investigated.

2. Theory

The quasistatic theory relates the line wing absorption $k(\bar{\nu})$ in a small energy interval $[\bar{\nu}, \bar{\nu}+\mathrm{d}\bar{\nu}]$ to the probability $W(r)\,\mathrm{d}r$ of finding the nearest perturber atom in a differential part $\mathrm{d}r$ at the internuclear distance r:

$$k(\bar{\nu})\,\mathrm{d}\bar{\nu} \sim W(r)\,\mathrm{d}r\,. \tag{1}$$

Here r is connected to the difference potential $V(r)$ by

$$h\,c\,\Delta\bar{\nu} = V(r) = V_u(r) - V_l(r) \tag{2}$$

where $V_u(r)$ and $V_l(r)$ are the adiabatic potentials of the upper and lower electronic molecular states

Reprint requests to Dr. K. Niemax, Institut für Experimentalphysik der Universität Kiel, Olshausenstr. 40–60, *D-2300 Kiel.*

respectively. Inserting formula (2) into formula (1) the absorption coefficient in the line wing is given by

$$k(\bar{\nu}) \sim h\,c\,W(r)\,\frac{1}{|\,\mathrm{d}V(r)/\mathrm{d}r\,|}\,. \tag{3}$$

Normalisation of the absorption line

$$\int k(\bar{\nu})\,\mathrm{d}\bar{\nu} = \frac{\pi\,e^2}{m\,c^2}\,N_\mathrm{A}\,f \tag{4}$$

and the binary interaction approximation

$$W(r)\,\mathrm{d}r = 4\,\pi\,r^2\,N_\mathrm{B}\exp\{-\Delta V_1(r)/k\,T\}\,\mathrm{d}r \tag{5}$$

leads to

$$k(\bar{\nu}) = \frac{4\,\pi^2\,r^2\,e^2\,h\,N_\mathrm{A}\,N_\mathrm{B}\,f}{m\,c}\,\frac{\exp\{-\Delta V_1(r)/k\,T\}}{|\,\mathrm{d}V(r)/\mathrm{d}r\,|}\,. \tag{6}$$

However, if more than two potentials (ground and excited state potentials) are responsible for the line wing the statistical weights of the molecular states must be inserted into formula (6). It is thus always possible to calculate the quasistatic line wings if the adiabatic potentials are known. It should be noted here that the oscillator strength f is assumed independent of internuclear distance, although slight changes with distance are possible (see e. g. Drullinger et al. [11]).

In comparisons of the theoretical wing and available experimental data it should be noted that the atoms are not fixed but in a state of motion during the absorption process. This causes – as is conspicuous –, a smearing out of the well known statellites which arise wherever the difference potentials have extrema [$\mathrm{d}V(r)/\mathrm{d}r = 0$; $k(\bar{\nu}) \rightarrow$ in formula (6)]. Because of heavy masses of Cs and Xe in our experiment the relative velocity of the atoms is low. So the effect of the smearing out is not so pronounced as in other alkali-noble gas systems.

Another aspect which has to be taken into account is that of non-adiabatic transitions between different molecular states during the collision. In the far and very far line wings these mixing collisions can be neglected in most cases.

If, as in the present experiment, the interacting atoms are not of the same species, the condition $N_\mathrm{A} \ll N_\mathrm{B}$ has to be fulfilled strictly. Otherwise, self-broadening effects have to be taken into account.

At low perturber density, in the region where two-body collisions predominate, the width and the shift of the line cores are proportional to the density of the perturbers and grow with the increasing principal quantum number. This is as predicted by impact theories [3]. The shapes of the line cores have to be Lorenzian.

When the perturber density is increased, two-body collisions become less and less important. The number of the perturber atoms within the electron orbit increases. Fermi [10] first showed that in this case the shift of the energy level is independent of the principal quantum number:

$$\Delta\bar{\nu} = \Delta\bar{\nu}_\mathrm{s} + \Delta\bar{\nu}_\mathrm{p} = \pm\frac{\hbar^2}{m}\,N_\mathrm{B}\,V\overline{\pi\,\sigma_0} - 10\,\alpha\,e^2\,N_\mathrm{B}^{4/3}\,. \tag{7}$$

Here $\Delta\bar{\nu}_\mathrm{s}$ is the shift due to the elastic scattering of the atomic electron in the excited state by the perturber atoms (density N_B) and $\Delta\bar{\nu}_\mathrm{p}$ is the shift due to the polarisation of the perturber particles within the electronic orbit. σ_0 is the cross section and α the polarizability of the foreign gas atom. For the high series members, the scattering contribution is usually predominant. Further considerations were made by Firsov [12] and by Alekseev and Sobel'man [13]. The examined the region of validity for Fermi's expresion for $\Delta\bar{\nu}_\mathrm{s}$ and the independence of scattering and polarisation effects respectively.

Only little is known about the change from two-body to many-body collisions and the connection with the statistical theory. It is the aim of this experimental investigation to provide more information about this transition region.

3. Experiment

The experimental set-up is shown schematically in Figure 1. The absorption measurements were performed using a 900 W Xe high-pressure or a 150 W halogen lamp as the continuous light source. After passing the Cs-Xe absorption tube (parallel beam)

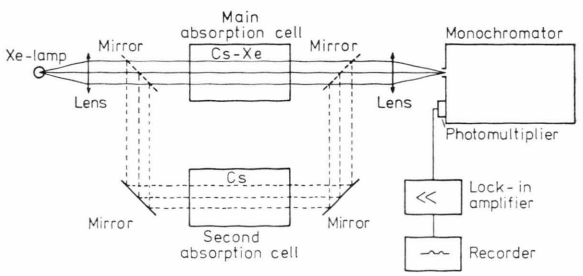

Fig. 1. The experimental set-up.

the light was focused onto the entrance slit of a high resolution Ebert-type scanning monochromator ($f=$ 10 m, optical band pass between 40 and 6 mÅ). At the exit slit the light was detected photoelectrically. After amplification the signal was registered on a strip-chart recorder. A systems of mirrors made it possible to use a second absorption tube containing Cs without a buffer gas and running at low Cs vapour densities for wavelength calibration.

The different absorption cells used were made of pyrex glass and had a length of 15 cm. Before filling with extremly pure Xe gas (pressure: 50, 200, 350 and 600 torr at room temperature) and sealing, the tubes were baked at about 360 °C under a vacuum of 10^{-6} torr for two or three days. Subsequently small Cs capsules were crushed inside the cells.

The absorption tube was located in a two-chamber-oven with separate heating systems. The upper chamber in which the observed part of the absorption cell was situated had a somewhat higher temperature than the lower chamber with the Cs bath in order to prevent cesium from covering the cell windows. The equilibrium vapour pressure above the liquid Cs was calculated with the help of the Taylor-Langmuir formula [14].

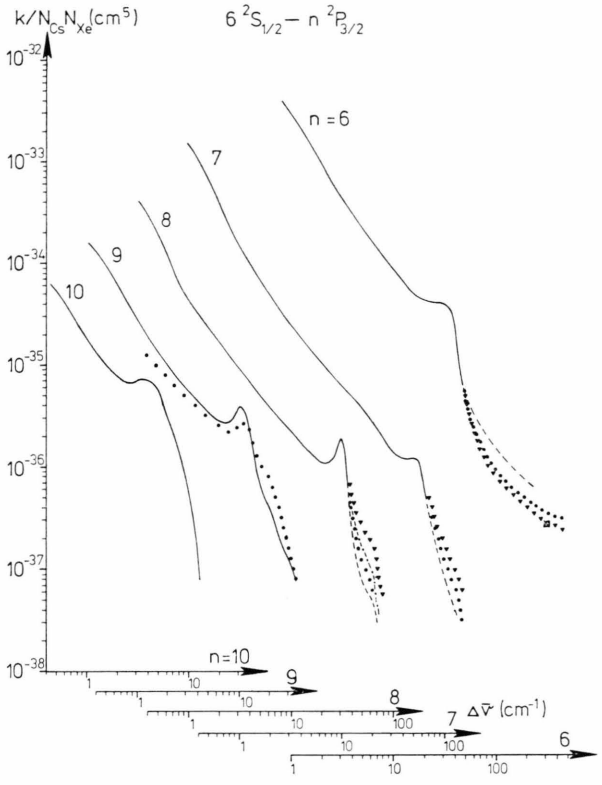

Fig. 2. The reduced absorption coefficients of the red wings of the $6\,^2S_{1/2}-n\,^2P_{3/2}$ lines as a function of the displacement from the undisturbed line centres. The solid curves represent the measured envelopes of all line wings at different Xe and Cs particle denisties. If there are deviations at different Xe densities it is marked by — — — ($N_{Xe}=1.63\times10^{18}$ cm^{-3}), ····· (6.41×10^{18} cm^{-3}), —·— (1.11×10^{19} cm^{-3}) and ▼▼▼ (1.9×10^{19} cm^{-3}). ■ is calculated from the emission measurements by Hedges et al. [4].

4. Results and Discussion

a) The Statistical Wings

The dependence of the absorption coefficient $k(\bar{\nu})$ on the distance from the undisturbed line centre $\Delta\bar{\nu}$ was derived from the measurements using the well-known relation

$$k(\bar{\nu}) = 1/L \ln[I_0(\bar{\nu})/I(\bar{\nu})] \qquad (8)$$

where $I_0(\bar{\nu})$ and $I(\bar{\nu})$ are the incident and transmitted light intensities and L is the length of the absorbing layer. Because of the high resolving power of the monochromator there was no serious distortion of the absorption profiles by the instrumental function. Figures 2 – 5 show the red and blue wings of the measured stronger (Fig. 2 and 4) and weaker (Fig. 3 and 5) components of the principal lines of Cs. The wings are presented in the usual log-log plot of the reduced absorption coefficient $k(\bar{\nu})/N_{Cs}N_{Xe}$ against the distance from the line centre $\Delta\bar{\nu}$. The solid curves represent the envelopes of all measured line wings at different Cs and Xe particle densities. Distinctions between measurements at different Xe particle densities are marked by broken and dotted curves. In the case of the resonance lines ($6\,^2S_{1/2}-6\,^2P_{3/2,1/2}$) there were also differences between the reduced absorption coefficients in the far wings depending on the Cs particle density. For clarity we do not show all measured far wings. Roughly speaking they were situated between the upper and the lower plotted wings. The dependence on the Cs particle density seems to indicate that self-broadening effects come into play. It is known (see e.g. Ref. [15]) that the cross section for self-broadening of the Cs resonance lines is large. Deviation should occur especially in the parts of the wings where the foreign gas broadening is weak and where the condition $N_{Cs} \ll N_{Xe}$ is not strictly fulfilled. The differences in the outer part of the red wings of the higher lines are only due to the Xe particle density. Note that the reduced absorption coefficient is the larger the higher the Xe particle density is. Because all measurements of the wing region of interest

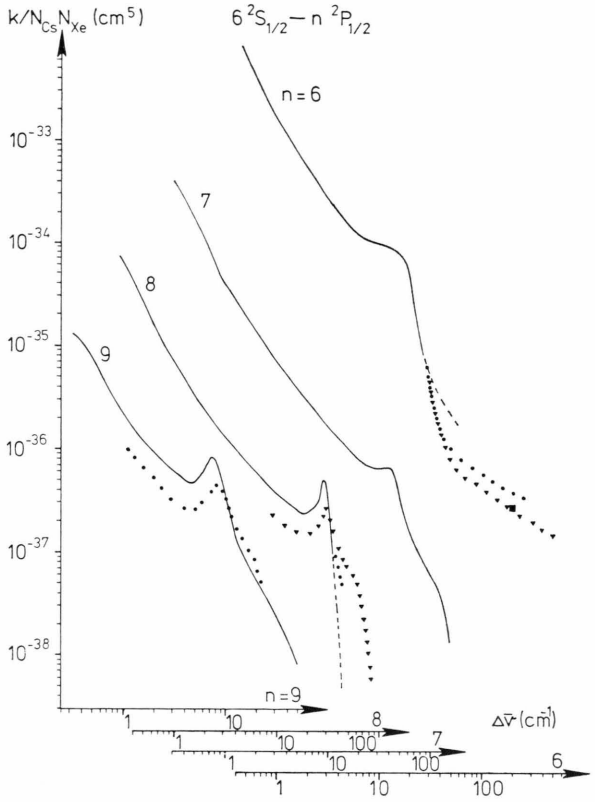

Fig. 3. The reduced absorption coefficients of the red wings of the $6\,^2S_{1/2}-n\,^2P_{1/2}$ lines. Further comments: see Figure 2.

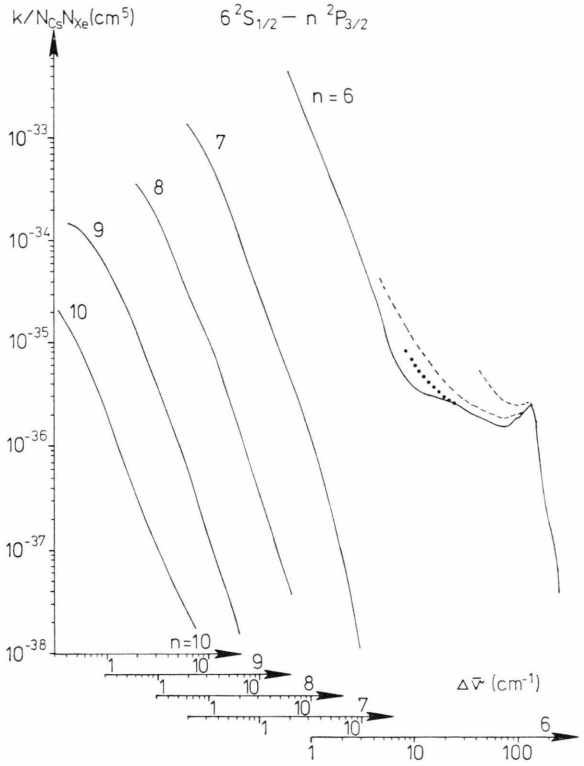

Fig. 4. The reduced absorption coefficients of the blue wings of the stronger components of the Cs principal series lines. Further comments: see Figure 2.

were done at nearly the same temperature, temperature dependence can be neglected in all considerations. The discrepancies appear to be a consequence of many-body interactions. Another interesting feature is a smeared out secondary satellite which has been observed on the red wings of all lines except the resonance lines. The higher the lines of the series the more pronounced these satellites are. The positions are roughly twice as far from line centre as the first satellite. Similar secondary satellites were found by McCartan and Hindmarsh [16] on the red wing of the K line 4047 Å disturbed by Kr and by McCartan and Farr [17] on the red wing of the 5896 Å resonance line disturbed by Kr and Xe. From the strong dependence of the shape of these secondary satellites on the foreign gas density (see Fig. 2 and 3) one may conclude that they arise from interaction involving more than two atoms. Most probable is a three-body interaction (Cs-Xe-Xe). This assumption is in line with recent calculations by Baylis [18]. Baylis shows that under certain circumstances three-body interaction excited-state potentials are the sum of two Cs-Xe potentials. Since the three-body ground state potential is also

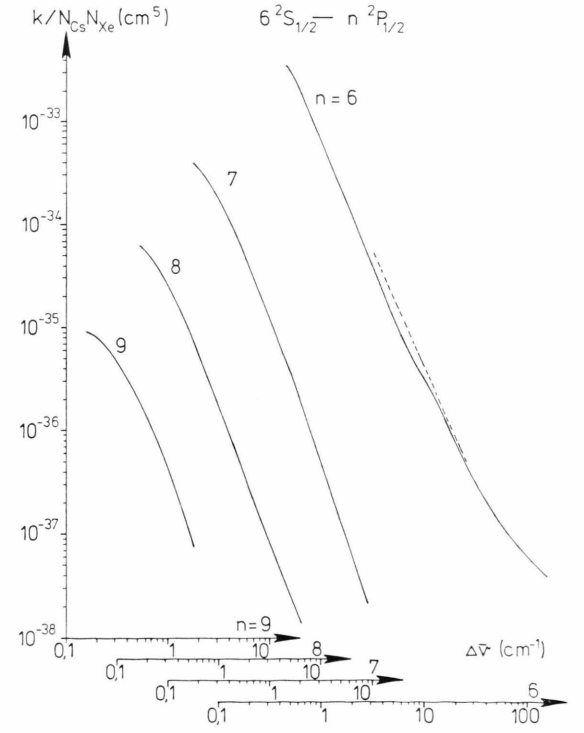

Fig. 5. The reduced absorption coefficients of the blue wings of the weaker lines. Further comment: see Figure 2.

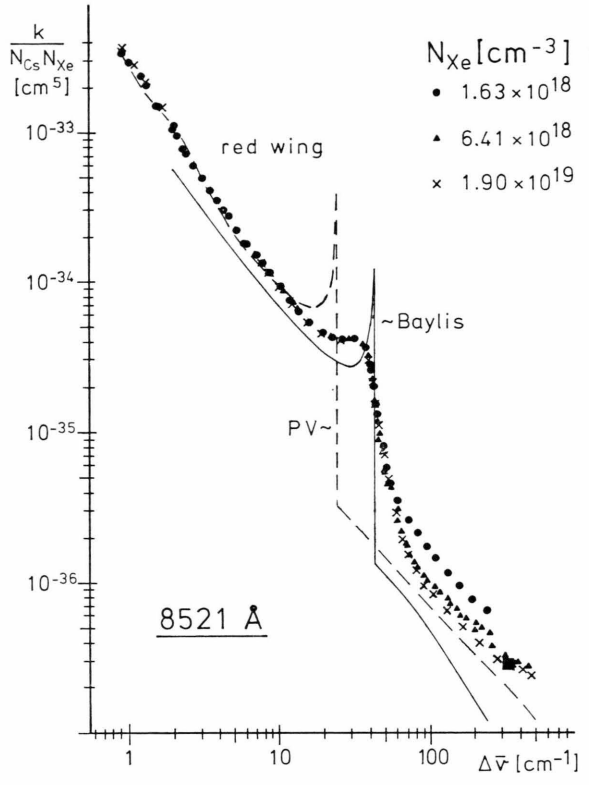

Fig. 6. Comparison between the experimental and the theoretical red wings of the 8521 Å line ($6\,^2S_{1/2}-6\,^2P_{3/2}$). The solid curve is based on Baylis' potentials [1] and the broken curve on the potentials of Pascale and Vandeplanque [2]. ■ is calculated from the emission measurements by Hedges et al [4].

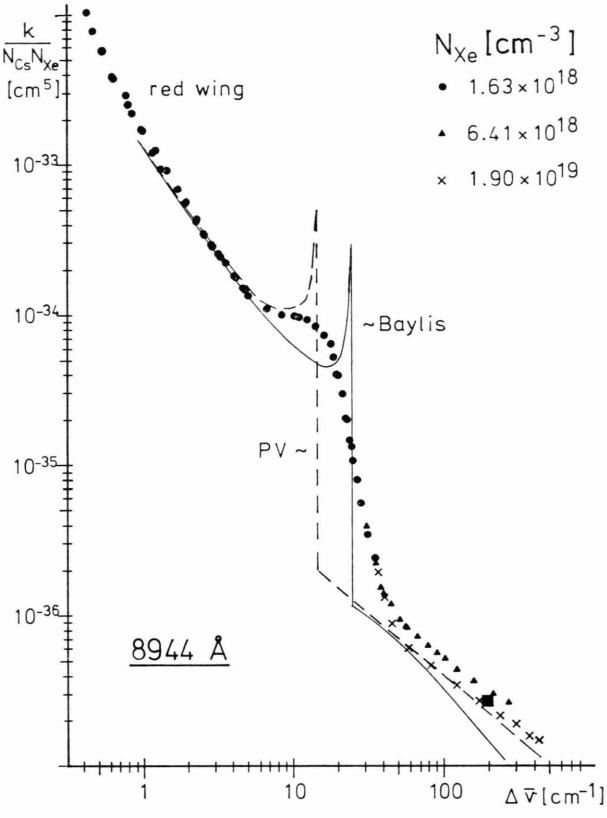

Fig. 7. Comparison between the experimental and theoretical red wings of the 8944 Å line ($6\,^2S_{1/2}-6\,^2P_{1/2}$). Further comments: see Figure 6.

twice the two-body ground state potential the extrema in the difference potentials are at the same internuclear distances for two and three-body interactions. On the other hand the difference in energy between the three and two-body difference potential at an extremum is twice as large. This is in line with the observed positions of the secondary satellites. Of course, the appearance of the secondary satellites depends on the foreign gas density and on the line which is observed. The higher the line in the series the earlier one can observe secondary satellites at a fixed perturber gas density because of the larger electron orbit of the excited Cs atoms. This can also be seen from Fig. 2 and 3.

The absorption lines $6\,^2S_{1/2}-9\,^2P_{3/2,1/2}$ and $6\,^2S_{1/2}-10\,^2P_{3/2}$ were only measured at the two lowest and the lowest Xe particle densities respectively. At higher densities the line centres shifted strongly towards longer wavelengths (transition region between the impact and Fermi theory, see next chapter); then it was no longer possible to measure the statistical wings. On the other hand the accuracy of these statistical wings should be used with care. It seems that the wings given by the full traces in the figures are not free from many-body interaction. Lower foreign gas densities are necessary in the experiment. But at those lower densities the condition $N_{Cs} \ll N_{Xe}$ would no longer be fulfilled, and self-broadening effects [19] have to be taken into account.

Because there are pronounced satellites on the red wings of the lines, one can be sure that the difference potentials are not monotonic functions of the internuclear separation. Therefore it is not possible to deduce them uniquely from the experiment. However, there is the possibility of checking theroretical potentials (see above). Inserting the difference potentials of Baylis [1] and Pascale and Vandeplanque [2] into formula (6) we have computed the quasi-static red and blue wings of the first doublets of the principal series. The calculations were made by inserting a typical temperature of 583 °K into the Boltzmann

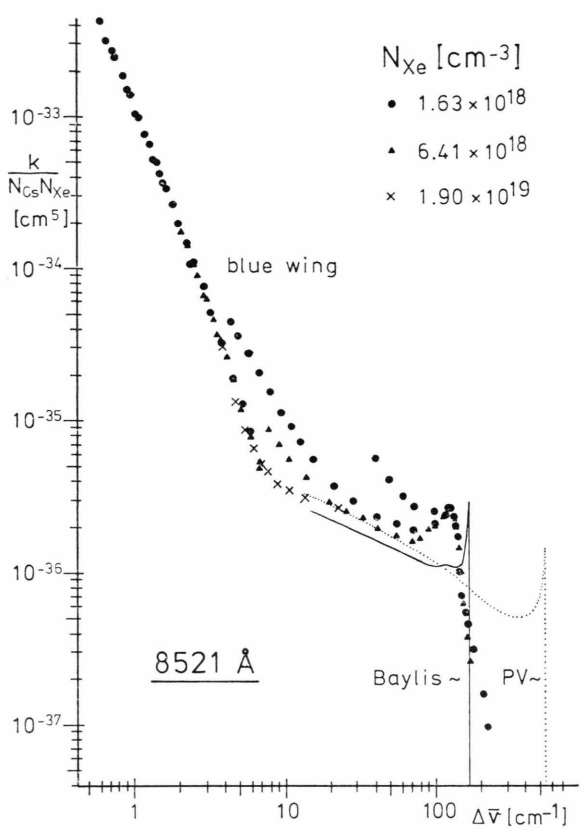

Fig. 8. Comparison between the experimental and theoretical blue wings of the 8521 Å line. The wings based on the potentials of Pascale and Vandeplanque are plotted as dotted and of Baylis as full curves.

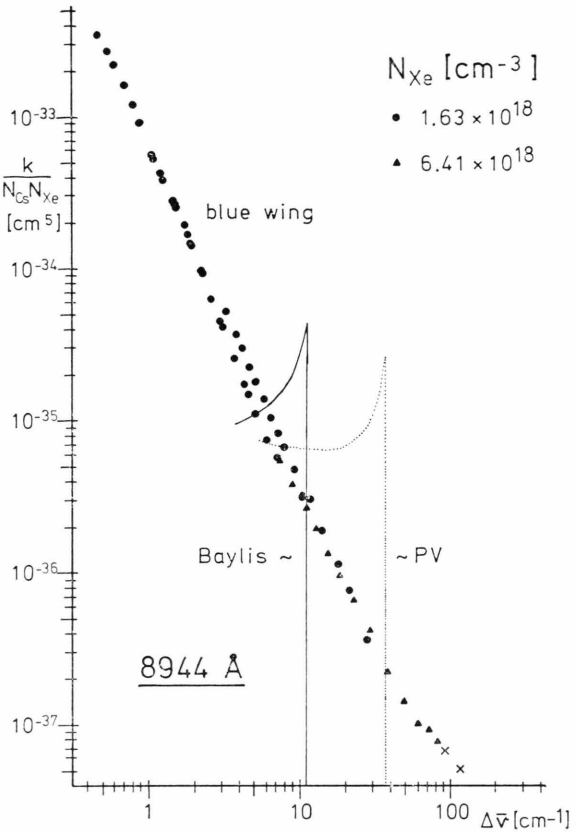

Fig. 9. Comparison between the experimental and theoretical blue wings of the 8944 Å line. Further comment: see Figure 8.

factor which gives the increased position probability in the attractive region of the lower potential. Only small parts of mostly outer quasi-static wings are influenced by the temperature in our case. In the calculations we used the theoretical oscillator strengths of Norgross [20] for the resonance lines and the experimental f-values of Pichler [21] for higher lines of the series. Figures 6 – 11 presents the comparisons between the theoretical and the experimental wings. Except for the positions of the satellites given by Pascale and Vandeplanque, an excellent agreement was found in the cases of the two red wings of the resonance lines (Fig. 6 and 7) and the blue wing of the 8521 Å line (Figure 8). Furthermore the values by Hedges et al.[4] (marked in Fig. 6 and 7) are well in line with our and the theoretical data. They were calculated from the normalized emission data ($T =$ 583 °K) given in the mentioned paper. In the case of the blue wing of the 8944 Å line, we did not observe the predicted satellite (Figure 9). Similar poor agreement between theory [2] and experiment was found for the wings of the 4555 and 4593 Å lines (Fig. 10 and 11). Because the theoretical blue satellites lie outside the impact regions [deviation of the wing ($k(\bar{\nu}) \sim \Delta\bar{\nu}^{-n}$, $n+2$) from Lorenzian wing ($k(\bar{\nu}) \sim \Delta\bar{\nu}^{-2}$) in the case of foreign gas broadening] they should have been observed. The comparison between the theoretical [2] and experimental wings of the next doublet (3876 and 3889 Å), not given in figures, resulted in even poorer agreement than in the case of the 4555 and 4593 Å lines.

b) The Shift of the Lines

In Fig. 12 the shift of the Cs principal series lines up to the 23rd member is plotted at four different Xe particle densities. Quite generally a distinction can be made between two regions of shift. The lower members of the series shift proportionally to the Xe density, but the values increase with increasing principal quantum number, whereas the shift of the

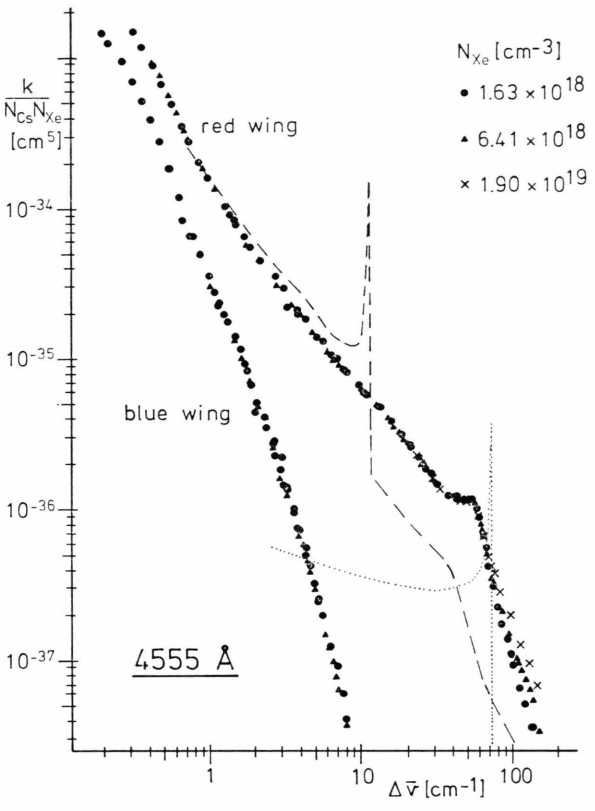

Fig. 10. Comparison between the experimental and the theoretical wings of the 4555 Å line. The quasistatic red (blue) wings based on Pascale's and Vandeplanque's potentials are given as broken (dotted) curves.

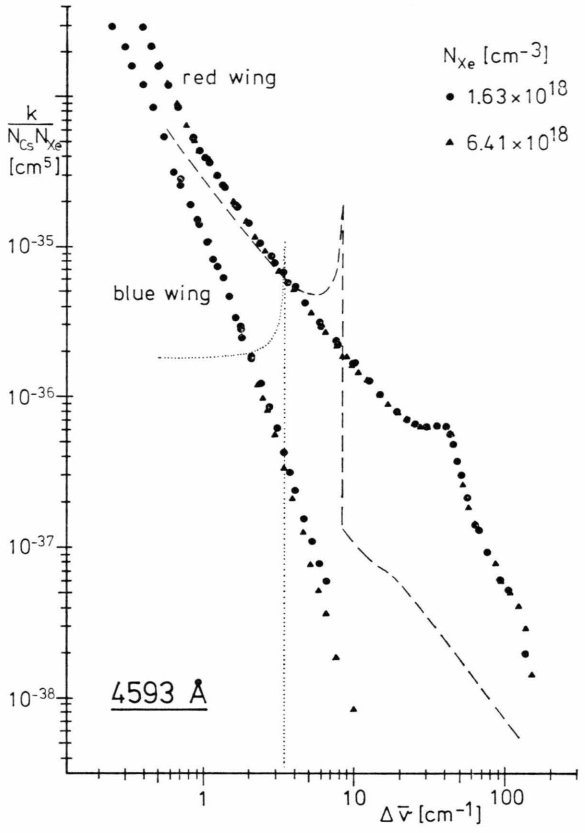

Fig. 11. Comparison between the experimental and the theoretical wings of the 4593 Å line. Further comments: see Figure 10.

higher members is proportional to the density, but in first approximation independent of the quantum number. This can also be seen from Fig. 13 and 14, where the shifts of the lower and of some higher lines are plotted against the particle density. The values presented in the figures are averaged values derived from up to 40 scans, and therefore the uncertainty is small. At low Xe particle densities where the impact broadening of the lower lines was still small it was possible to measure the shift of the hyperfine components as the shift of the centre of gravity at half-height. At higher densities the hyperfine components become more and more blended. In this case we found the centre of the line by taking into account the known intensity ratio (9:7) of the two groups of hf-components due to the splitting of the $6\,^2S_{1/2}$ ground state. If the lines were strongly asymmetric in the region of half-height we measured the shift of the maximum absorption of the lines. This had to be done for the shift of the lines which were neither described by impact nor by the Fermi theory (transition region, see Figure 15). In Table 1 and 2 the measured shift rates $\Delta\bar{\nu}/N_{Xe}$ are presented in the region of validity of the impact and of Fermi's theory. The total estimated error is mainly effected by the uncertainty in the Xe particle density (about 2%) and by the evaluating procedure of the shift values mentioned above. The scatter in our experimental data was low (1 – 2.5%). Apart from the present results the shift data available in literature are also given in Table 1. Good (line: 6S-6P) and poorer agreement (lines: 6S-7 and 8P) was found between our measurement and the predicted shift rates by Kielkopf [22]. The values of Kielkopf, who inserted semiempirical potentials (C_6, C_8, C_{12}) into his calculations, had been adjusted to our experimental temperatures. The theoretical values given by Granier et al. [7] based on the adiabatic potentials of Pascale and Vandeplanque [2] are about 30% smaller than ours. Because

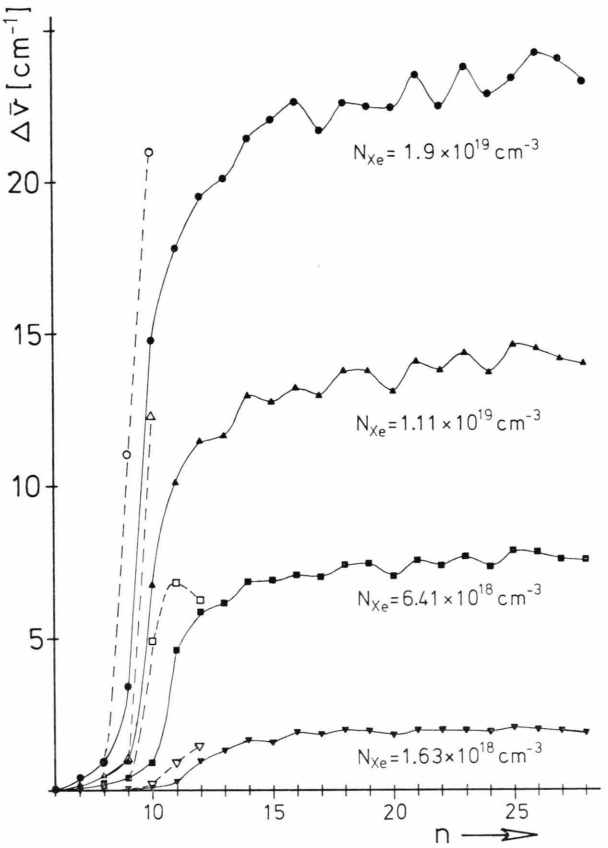

Fig. 12. The shift of Cs principal series lines caused by Xe. Full and open marks signify the shift values of the stronger and weaker components respectively.

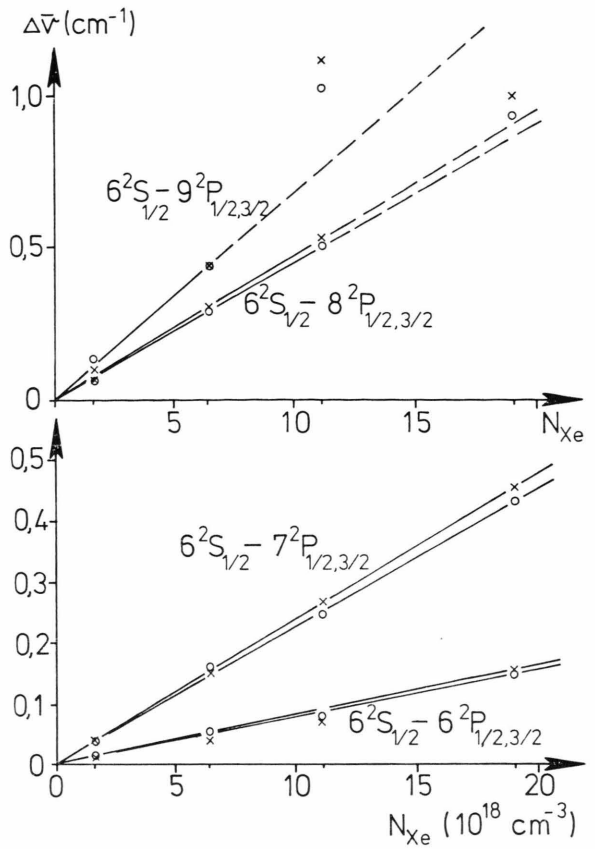

Fig. 13. The shift of line centres at half-height as a function of the Xe particle density. (o) refer to the stronger and (×) to the weaker lines.

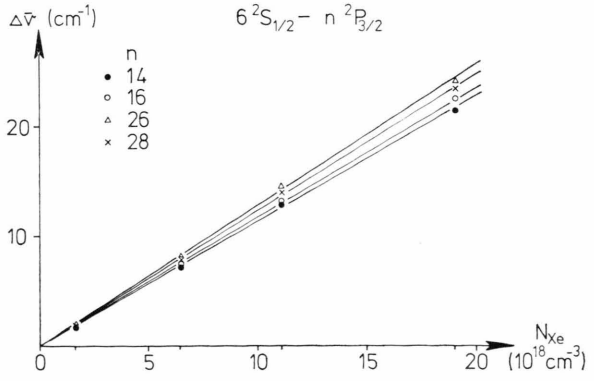

Fig. 14. The shift of some higher members of the principal series lines as a function of the Xe particle density.

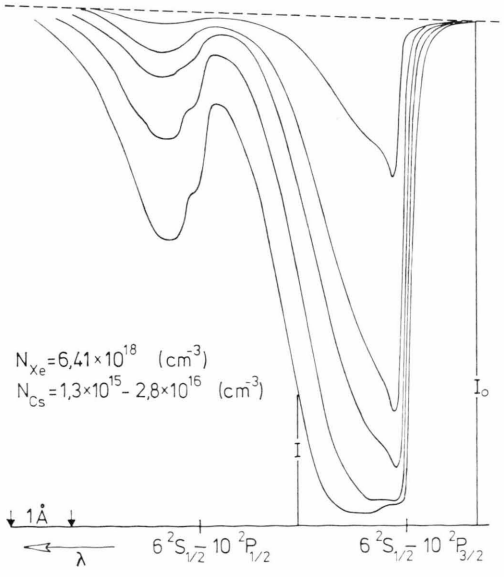

Fig. 15. Experimental traces of the perturbed 10th doublet of the Cs principal series lines.

	Shift rates $\Delta\bar{\nu}/N$ [10^{-20} cm^2]				
$6\,^2S_{1/2}$-	This work	T [°K]	Kielkopf [22]	Granier [7]	Smith [23]
$6\,^2P_{3/2}$	0.71 ± 0.04	303	0.702	0.509	
$6\,^2P_{1/2}$	0.75 ± 0.04			0.52	
$7\,^2P_{3/2}$	2.26 ± 0.08	373	1.82		
$7\,^2P_{1/2}$	$2.4\ \pm0.08$				1.63
$8\,^2P_{3/2}$	4.56 ± 0.14	424	2.94		
$8\,^2P_{1/2}$	4.76 ± 0.14				
$9\,^2P$	6.97 ± 0.6	473			

Table 1. The comparison of the shift rates. The theoretical rates by Granier et al.[7] are not $T^{0.3}$ corrected because the temperature is not given in that paper.

Table 2. The shift rates of the higher Cs principal series lines perturbed by Xe. The total estimated error does not significantly exceed 3%.

$6\,^2S_{1/2}-n\,^2P_{3/2}$ n	$\Delta\bar{\nu}/N$ [10^{-18} cm^2]	$6\,^2S_{1/2}-n\,^2P_{3/2}$ n	$\Delta\bar{\nu}/N$ [10^{-18} cm^2]
14	1.14	21	1.23
15	1.12	22	1.21
16	1.17	23	1.25
17	1.15	24	1.20
18	1.21	25	1.27
19	1.20	26	1.27
20	1.15	27	1.24
		28	1.22

we do not know the temperatures inserted in their calculations, we could not make the $T^{0.3}$ correction. Therefore an exact comparison is not possible. Only one experimental value is available in the literature (Smith [23]). The shift rate of the 4593 Å line given by this author was converted to our experimental conditions (mean temperature: 373 °K). The agreement is not satisfactory.

The transition from the region of impact theory to the region described by Fermi's theory occurs where the mean interatomic distance is roughly equal to the sum of the mean radii of the electron orbits of the excited Cs atom and the ground state Xe atom. Deviations of the linearity of the shift with increasing particle density can be seen at 1.11×10^{19} and 1.9×10^{19} cm^{-3} for the $6\,^2S_{1/2}-9\,^2P_{1/2,3/2}$ and the $6\,^2S_{1/2}-8\,^2P_{3/2,1/2}$ lines respectively (see Figure 13). The mean interatomic distances are 23.3 Å (1.9×10^{19} cm^{-3}) and 27.8 Å (1.11×10^{19} cm^{-3}). The mean radii of the 8P and 9P atom are 15.9 and 24.3 Å respectively whereas the Xe radius is about 1 Å (see e. g. Ref. [1]). The Cs radii were calculated using the approximate formula given by Unsöld [24]

$$\bar{r}_e = a_0/\sqrt{2}\,n^*\,[5\,n^{*2}+1-3\,l(l+1)\,]^{1/2}\,.$$

From Fig. 12 it can be seen that the higher lines reach their transition region at lower particle densities.

It is interesting to note that the lines of the doublets show a different shift-behaviour in the region of change between the theories. The shift of the weaker lines is larger than that of the stronger ones. This is just the opposite behaviour as in the case of Cs-Ar [25]. In Fig. 15 experimental traces of the lines 3477 and 2480 Å are given for a fixed Xe particle density (6.41×10^{18} cm^{-3}). The Cs particle density was varied between 1.3×10^{15} and 2.8×10^{16} cm^{-3}. The lines are strongly asymmetric. On the red wing of the stronger component we see the first satellite which is smeared out. At low Cs density the impact centre of the line which is shifted 95 mÅ is predominant. With increasing Cs particle density the absorption coefficient grows faster in the line wing than in the line centre. Finally at 2.8×10^{16} cm^{-3} the absorption coefficient is largest in the region of the satellite. The feature of the weaker line is quite different. From the beginning at low Cs particle densities the strongest absorption is in the region of the satellite. The remaining impact centre is still indicated as a shoulder in the wing (approximative shift: about 110 mÅ). Note that the maximum absorption of this line is shifted about 595 mÅ from the centre of the undisturbed line. This shift is of the same order as the shift of the stronger component at high Cs particle densities (about 590 mÅ). The different behaviour of both lines could be connected with the fact that the $P_{3/2}$ atomic level is split up into two excited molecular potentials ($\Sigma_{1/2}$ and $\Pi_{3/2}$) whereas the $P_{1/2}$ state is non-degenerate ($\Pi_{1/2}$).

Because the oscillator strengths of the weaker lines decrease faster than those of the stronger lines with increasing main quantum number [20, 21] and because of the broadening of the stronger components the shifts of the higher $6\,^2S_{1/2} - n\,^2P_{1/2}$ lines could not be measured. However, it appears to be a similar shift behaviour of both components at higher quantum numbers (see Figure 13). As mentioned above, the shift of all higher lines depends linearly on the Xe particle density (Figure 14). The experimental shift rates of these lines with the total estimatel errors are presented in Table 2. The reason for the small differences in the shift (ondulation in in Fig. 13) which are outside the experimental error is not known. The agreement between our data and the asymptotic shift rate of high Cs lines found by Tan and Ch'en [26] ($\Delta\bar{\nu}/N = 1.3 \times 10^{-18}\,\mathrm{cm}^2$) is satisfactory.

5. Conclusion

In this paper it was shown that the investigation of the statistical wings of pressure broadened lines is a useful tool for checking theoretical calculations of adiabatic potentials. Experiments of this kind can aid theoreticians in improving their calculations in some cases. On the other hand the experimentalists should be encouraged to undertake further line broadening investigations of gas systems for which theoretical potentials are available.

Some indications of many-body interaction were found in the far wings of the higher lines of the series. Of course, these effects do not allow a direct comparison with the theoretical quasistatic wings based on the binary-interaction approximation. Furthermore it can be seen from the present experiment that many-body interactions dominate the whole line if the shift of the line centre can no longer be described by the impact theory (region of transition from the impact to Fermi's theory). Thus the measurement of the shift should be a good test of the two-body interaction.

We thank Prof. J. Richter for encouragement and Prof. W. E. Baylis for providing the unpublished results of the Cs-Xe potentials and for helpful conversation.

[1] W. E. Baylis, J. Chem. Phys. **51,** 2665 [1969].
[2] J. Pascale and J. Vandeplanque, J. Chem. Phys. **60,** 2278 [1974] and Commisariat a l'Energie Atomique Report (V: cesium) [1974].
[3] S. Y. Ch'en and M. Takeo, Rev. Mod. Phys. **29,** 20 [1957].
[4] R. E. M. Hedges, D. Drummond, and A. Gallagher, Phys. Rev. A **6,** 1519 [1972].
[5] J. Losen and W. Behmenburg, Z. Naturforsch. **28 a,** 1620 [1973].
[6] C. L. Chen and A. V. Phelps, Phys. Rev. A **7,** 470 [1973].
[7] R. Granier, J. Granier, and F. Schuller, J. Q. S. R. T. **16,** 143 [1976].
[8] W. Behmenburg, J. Q. S. R. T. **4,** 177 [1964].
[9] W. R. Hindmarsh, A. D. Petford, and G. Smith, Proc. Roy. Soc. A **297,** 296 [1967].
[10] E. Fermi, Nuovo Cimento **11,** 157 [1934].
[11] R. E. Drullinger, M. M. Hessel, and E. W. Smith, National Bureau of Standards Monograph 143 [1975].
[12] O. B. Firsov, J. Exp. Theor. Phys. **21,** 627 [1951] and **21,** 634 [1951].
[13] V. A. Alekseev and I. I. Sobel'man, J. Exp. Theor. Phys. **49,** 1274 [1965] and Sov. Phys. J. Exp. Theor. Phys. **22,** 822 [1966].
[14] J. B. Taylor and I. Langmuir, Phys. Rev. **51,** 753 [1937].
[15] K. Niemax and G. Pichler, J. Phys. B: Atom. Molec. Phys. **7,** 2355 [1974].
[16] D. G. McCartan and W. R. Hindmarsh, J. Phys. B: Atom. Molec. Phys. **2,** 1396 [1969].
[17] D. G. McCartan and J. M. Farr, J. Phys. B: Atom. Molec. Phys. **9,** 985 [1976].
[18] W. E. Baylis, private communication.
[19] K. Niemax and G. Pichler, J. Phys. B: Atom. Molec. Phys. **8,** 2718 [1975].
[20] D. W. Norcross, Phys. Rev. A **7,** 606 [1973].
[21] G. Pichler, J. Q. S. R. T. **16,** 147 [1976].
[22] J. W. Kielkopf, J. Phys. B: Atom. Molec. Phys. **9,** L 547 [1976].
[23] G. Smith, J. Phys. B: Atom. Molec. Phys. **8,** 2273 [1975].
[24] A. Unsöld, Physik der Sternatmosphären, Springer-Verlag, Berlin 1968, Chapter 11.
[25] M. A. Mazing and N. A. Vrublevskaya, Sov. Phys. J. Exp. Theor. Phys. **23,** 228 [1966].
[26] D. K. L. Tan and S. Y. Ch'en, Phys. Rev. A **2,** 1124 [1970].